MAPPING IMPERVIOUS SURFACE AREA USING HIGH RESOLUTION IMAGERY: A COMPARISON OF OBJECT-BASED AND PER PIXEL CLASSIFICATION

Fei Yuan, Assistant Professor
Department of Geography
Minnesota State University, Mankato
Armstrong Hall 7F
Mankato, Minnesota 56001
fei.yuan@mnsu.edu

Marvin E. Bauer, Professor
Department of Forest Resources
University of Minnesota
1530 Cleveland Avenue North
St. Paul, MN 55108
mbauer@umn.edu

ABSTRACT

Impervious surface area is a key indicator of environmental quality. Satellite remote sensing of impervious surface has focused on subpixel analysis via various forms of statistical estimation, subpixel classification, and spectral mixture analysis, using medium resolution Landsat TM or ETM+ data. Maps of impervious surface area from these studies provide useful inputs to planning and management activities at city to regional scales. However, for local studies, large-scale, higher resolution maps are preferred. This study investigates digital classification techniques of mapping of impervious surface area using high resolution Quickbird satellite data. Two methods – object-based and per pixel classification – are explored and compared. The results provide information for accurate impervious surface mapping and estimation in high resolution imagery.

INTRODUCTION

Impervious surfaces, including building rooftops, streets, highways, parking lots, and sidewalks, which water cannot infiltrate, directly affect the amount of runoff to streams and lakes and non-point source pollution and water quality, and the aesthetics of landscapes (Dougherty et al., 2004). Accurate measurement of impervious surface area provides an essential indicator of environmental quality and valuable input to planning and management activities (Schueler, 1994). Traditional ground surveys and aerial photography interpretation are the most accurate methods, but they are not time effective. Alternatively, the decreasing costs and increasing availability of digital imagery have led to more and more successful programs of impervious surfaces mapping by classification of digital satellite data.

Satellite remote sensing of impervious surface has focused on subpixel analysis using Landsat TM or ETM+ data with 30-meter resolution. One of the major subpixel analysis approaches is spectral mixture analysis (SMA) which estimates percent impervious surface by analyzing various vegetation-impervious-soil endmembers (Adams et al., 1995; Lu and Weng, 2004; Wu, 2004; Wu and Murray, 2003). Another method is regression, either statistical regression which relates %ISA to "tasseled cap" greenness (Bauer et al., 2004; Yuan et al., 2005) or regression tree (Yang et al., 2003). In addition, ERDAS/Imagine subpixel classification which uses an intelligent background estimation process to remove other materials in the pixel and calculate the amount of impervious surface percent have been investigated by Ji and Jensen (1999) and Civico et al. (2002).

Results from these studies have provided valuable inputs to planning and management activities at city to regional scales. However, for large-scale local studies, higher resolution data are preferred. Currently, there are two major commercial sources of imagery. IKONOS data from Space Imaging launched in 1999 and Quickbird imagery from DigitalGlobe launched in 2001. Digital classifications, especially urban impervious mapping, using these high resolution satellite data are limited. However, Sawaya et al. (2003) mapped impervious surfaces for Eagan, Minnesota using IKONOS data. Small (2003) used IKONOS imagery to quantify the spatial and spectral characteristics of urban reflectance in 14 urban areas worldwide. In related studies of the effects of shadowing which can be a significant component of high resolution images, Asner and Warner (2003) used 44 IKONOS images to quantify the spatial variation of canopy shadow fraction across a broad range of forests in the Brazilian Amazon and savannas in the Brazilian Cerrado. Nevertheless, to date, automatically extracting urban features from high-resolution remote sensing data is still a challenging task. Particularly, building and tree shadows in high resolution images have presented a serious problem for digital classification (Niemeyer and Canty, 2001).

his study examines digital land use exaction, especially urban impervious classification techniques in Quickbird imagery. Two methods – object-based and per pixel classification – are explored and compared. While the traditional per-pixel classification methods are based on the spectral-radiometric information of individual pixels, the object-oriented approach provides unique capabilities to incorporate large-scale textural and contextual information as well as numerous object-based features in the classification process. Therefore the object-based classification has the potential to enhance the accuracy of the classification. However, previous studies show some inconsistent results. Some studies have found a significantly higher accuracy for the object-oriented approach (Benz et al. 2003; Schwarz et al., 2000; Wang et al., 2004), while other investigations reported the two approaches produced similar results with comparable accuracy (Willhauck, 2000; Sun, 2003). The objectives of this study include: (1) comparison of the pixel-based classification to the object-based approach; (2) evaluation of how noises such as shadow in Quickbird images can be handled in digital classification process; and (3) analysis of what extent Quickbird data can be used to map urban impervious structures.

METHODS

Study Area and Data Preparation

Our study focuses on a 2.1 km by 1.7 km area surrounding the Minnesota State University, Mankato campus. The central coordinates are (44.147° N, 93.992° W). Given the varied land covers it includes, it provides a good test site for the purpose of exploring classification techniques.

Quickbird imagery acquired on October 6, 2003 at 16:55 p.m. was obtained from the Digital Globe archive collection. The data were recorded in 11 bits and were radiometrically and geometrically corrected. The image includes four multispectral bands at 2.4-m resolution and one panchromatic band at 0.6-m resolution. The sun azimuth and elevation angle were 158.1 and 38.5 degrees and the satellite azimuth and elevation view angles were 27.7 and 76.3 degrees.

The Quickbird data were first converted from GeoTiff file to ERDAS/Imagine format, and then reprojected from original UTM (spheroid WGS84, zone 15), Datum WGS84 system to UTM (spheroid NAD83, Zone 15), and Datum GRS 1980 system to match that of the ancillary data. The primary ancillary data used was the National Agriculture Imagery Program (NAIP) color digital ortho-rectified aerial photography, acquired in the summer of 2003 (June 26), by the U.S. Department of Agriculture. This color aerial imagery was utilized as visual reference for selecting training and testing samples.

Classification Scheme and Sample Extraction

Digital classifications were applied to the Quickbird imagery to first classify the data into generalized level-1 land cover classes. In particular, the data were classified into five classes – impervious surface, forest, water, non-forested rural, and shadow. Next, shadow was assigned to the other four classes by further analysis and classification. Finally, all the land covers were recoded into two groups, impervious and non-impervious. Two software packages – ERDAS Imagine 8.7 and eCognition 4.0 – were used to perform per-pixel classification and object-oriented classification, respectively.

Two sets of training samples were manually delineated for the per-pixel maximum likelihood classification in ERDAS Imagine and for the object-oriented classification in eCognition. The reason for using different training sets for the two methods is because the object-based approach using the nearest neighbor classifier requires fewer training samples than pixel-based training since one sample object includes several to many typical pixel samples and their variations; otherwise the heterogeneous character of the samples will not be fully considered (Baatz at el., 2004). However, for better comparison, the same set of accuracy assessment samples was developed based on the image objects in eCognition and was applied in both methods. All training and accuracy assessment data were checked against the 1-m NAIP color aerial imagery. The locations of training and accuracy assessment samples were selected randomly and distributed evenly across the study area.

Per-pixel Maximum Likelihood Classification

In this study, the maximum likelihood classifier (MLC) of ERDAS Imagine was utilized for the per-pixel classification. In MLC, the probability of a given pixel in a category is defined from the density likelihood function for a normal distribution that represented by the mean vector and the covariance matrix of classes. Although MLC is based solely on spectral information of remote sensing data, it has been established as the standard statistical method for digital image classification for it advantage from the view point of probability theory (Chan et al., 2001).

To differentiate different types of shadow in the second stage analysis, a specialized filtering function named neighborhood function was performed, in which each shadow pixel was analyzed with the pixels in its 5 x 5 neighborhood and was replaced by the majority class of its neighborhood.

Object-oriented Classification

The first step in eCognition's object-based classification procedures is multiresolution segmentation which extracts image objects at modifiable scale parameters, single layer weights and the mixing of the homogeneity criterion concerning color and shape. Next, a nearest neighbor classifier is trained by sample image objects and finally classifies image objects in a given feature space as well as automatically generates multidimensional membership functions (Baatz et al., 2004).

The outcome of segmentation is directly related to several adjustable criteria – scale parameter, color, and shape – defined by users. In particular, the scale parameter is a measure for the maximum change in heterogeneity that may occur when merging two image objects. A larger scale parameter value leads to bigger objects and vice versa. Adjusting the shape factor will also affect the overall fusion value that is computed based on both spectral heterogeneity and the shape heterogeneity. Therefore, how to choose an optimal scale parameter and shape factor is critical to the quality of classification. To set the appropriate objects for use and to evaluate how classification accuracy changes when adjusting these two criteria, different scale parameters ranging from 5 to 50 and shape factors ranging from 0.1 to 0.9 were utilized to classify the data.

Besides the scale parameter and shape factor, the result of object-oriented classification is also dependent on the object-based metrics, including measures of texture, length, and shape as well as measures of spatial relationships to other super-, sub-, and neighboring objects, utilized in the classification process. In this study, two additional object-based metrics – "Ratio of Band 1", and "Ratio of Band 4" – were selected and tested. The "Ratio of Band L" is the band L mean value of an image object divided by the sum of all spectral band mean values. For impervious surfaces, the "Ratio of the Band 1" (blue band) is comparatively high, and the "Ratio of Band 4" (near infrared band) is relatively low, which may help differentiate impervious areas from the other land cover classes. To determine if the use of the metrics would improve the classification, step-wise classifications by adding these metrics were also performed.

To distinguish special types of shadow, class-related features – relative to their adjacency forest or impervious – were added in the second level classification. For example, if more than 55% of the relative border of the shadow object was impervious or forest, then the shadow object was assigned a new value of impervious or forest. Otherwise, the shadow was classified as non-forest.

RESULTS

Classifications were first implemented with two different band selections – multispectral bands with and without the panchromatic band. However, the preliminary results indicated the inclusion of panchromatic bands did not improve but slightly decreased the visual effects and overall accuracies for both maximum likelihood and object oriented approaches. Therefore, the panchromatic band was excluded in the final analysis and classifications.

Our study indicates that the results of the object oriented classification are dependent on the user defined values of scale parameter and shape factor. In particular, the overall accuracy of the object-based classification reaches the highest point when the shape factor equals to 0.3 and then it trends down to the lowest when shape factor weight is 0.9. However, different land cover classes show different change trends over the shape factor. For example, the accuracy of water is not affected by changing the value of shape factor while the impervious class shows steadily decreasing accuracy with increases in the shape factor value. Similarly, the overall performance of the classification shows a clear change tendency with alterations of the scale parameter. At a scale parameter equal to 5 the overall accuracy is 86%, then increases to its highest value of 91% when scale parameter increases to 20, and finally drops to about 82% when the scale parameter increases to 50 (Figure 1). From Figure 1 we can see, for this specific study, the optimal shape factor and scale parameter are 0.3 and 20, respectively.

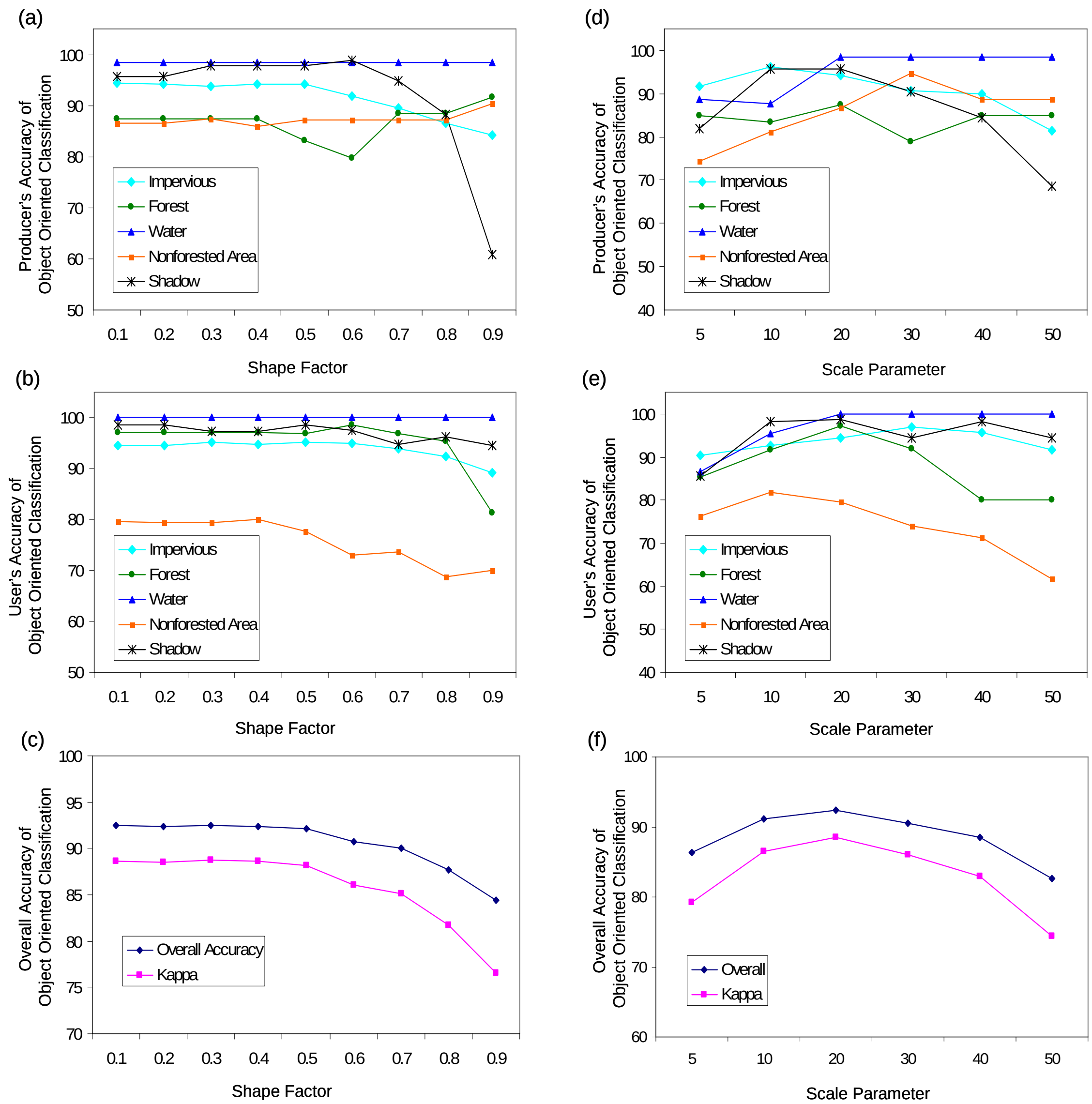

Figure 1. Effects of shape factor (a–c) and scale parameters (d-f) on the accuracy of object oriented classification.

The results also demonstrate that adding the two extra feature variables of “Ratio of Band 4” and “Ratio of Band 1” did affect the classification accuracy. While the Kappa value increases 1% when adding the “Ratio of Band 1” only, the overall accuracy decreases 3% by adding the “Ratio of Band 4”. This is probably because the “Ratio of Band 4” shows similar values for some forests and non-forested vegetation, which lead to decreased accuracy for forest and non-forested areas. Nonetheless, when both ratios of band 1 and band 4 were added, the classification results increased about 2% (Table 1).

The pixel-based classification showed some considerable speckling of impervious areas throughout the study area (Figure 2), whereas the object-based classification map is much more homogeneous. Accuracy of the classification results from these two approaches has also been assessed by creating error matrix using the same test area as reference data. Comparison of the accuracy assessment results shows that object-oriented image analysis has a slightly higher overall accuracy and higher individual land cover class accuracy for each classified land cover class (Tables 2 and 3).

Table 1. Summary of Landsat classification accuracies (%) for object oriented classifications with different feature variables utilized.

	Mean Brightness of All Bands		Mean Brightness of All Bands; Ratio of Band 1		Mean Brightness of All Bands; Ratio of Band 4		Mean Brightness of All Bands; Ratio of Band 1; Ratio of Band 4	
Land Cover Class	**Producer**	**User**	**Producer**	**User**	**Producer**	**User**	**Producer**	**User**
Impervious	94.4	93.2	92.1	94.4	94.2	93.7	94.2	94.5
Forest	97	81.3	87.4	97.2	97	65.3	87.4	97.2
Water	98.5	100	98.5	94.7	98.5	100	98.5	100
Non-forested	71.9	83	86.6	76.7	55.3	76.7	86.6	79.5
Shadow	95.7	96.7	95.7	98.7	97.7	98.7	95.7	98.7
Overall	90.7		91.3		87.6		92.4	
Kappa	85.9		86.9		81.3		88.5	

In the level-2 classification, shadow was further classified to imperious or non-imperious area using class-related features. Final impervious maps are generated by combining the "shadowed" imperious areas with the level-1 impervious class (Figure 3). In general, the two impervious classifications look very comparable. While the object-based map seems smoother, the maximum likelihood classification shows clearer urban infrastructure patterns, especially for single family residential areas. A separate accuracy assessment using 200 randomly sampled impervious points indicated a 93% and 94% overall accuracies for the impervious/non-impervious maps generated from the maximum likelihood classification and the object oriented method, respectively.

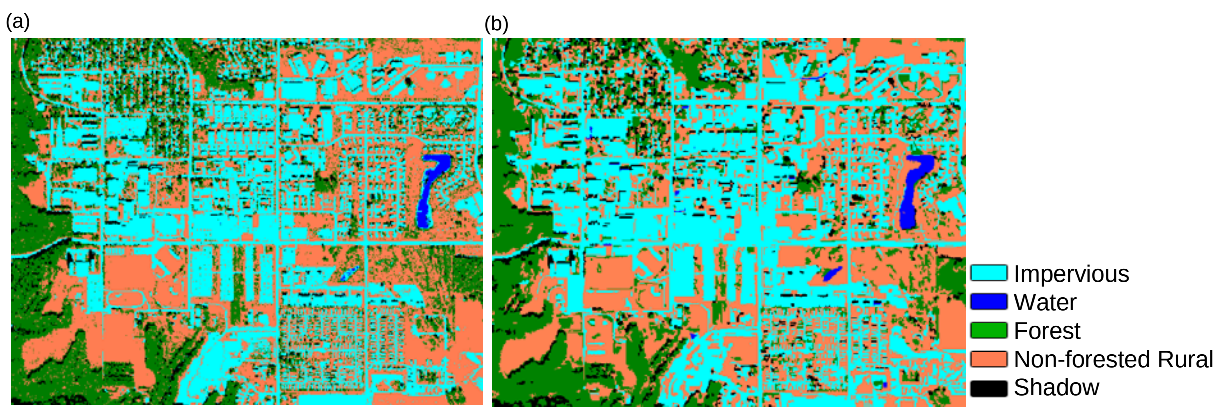

Figure 2. Comparison of level-1 (a) maximum likelihood and (b) object oriented classifications.

Table 2. Error matrix of land cover classification for per-pixel maximum likelihood classification.

Reference Class	Per-pixel Maximum Likelihood Classification					
	Impervious	Forest	Water	Non-forest	Shadow	Producer's Accuracy (%)
Impervious	7692	6	143	523	69	91.2
Forest	46	1502	0	280	43	80.3
Water	0	0	762	0	0	100.0
Non-forest	590	303	0	2320	0	72.2
Shadow	41	0	36	0	1739	95.8
User's Accuracy (%)	91.9	82.9	81	74.3	94.0	
Overall accuracy (%) = 87.1 Kappa (%) = 80.4						

Table 3. Error matrix of land cover classification for object-based land cover classification.

Reference Class	Object-Oriented Classification					
	Impervious	Forest	Water	Non-forest	Shadow	Producer's Accuracy (%)
Impervious	7904	3	0	490	36	93.7
Forest	0	1569	0	226	0	87.4
Water	0	0	935	0	14	98.5
Non0forest	399	0	0	2752	0	87.3
Shadow	0	43	0	0	1799	97.7
User's Accuracy (%)	95.2	97.2	100	79.4	97.3	
Overall accuracy (%) = 92.5 Kappa (%) = 88.7						

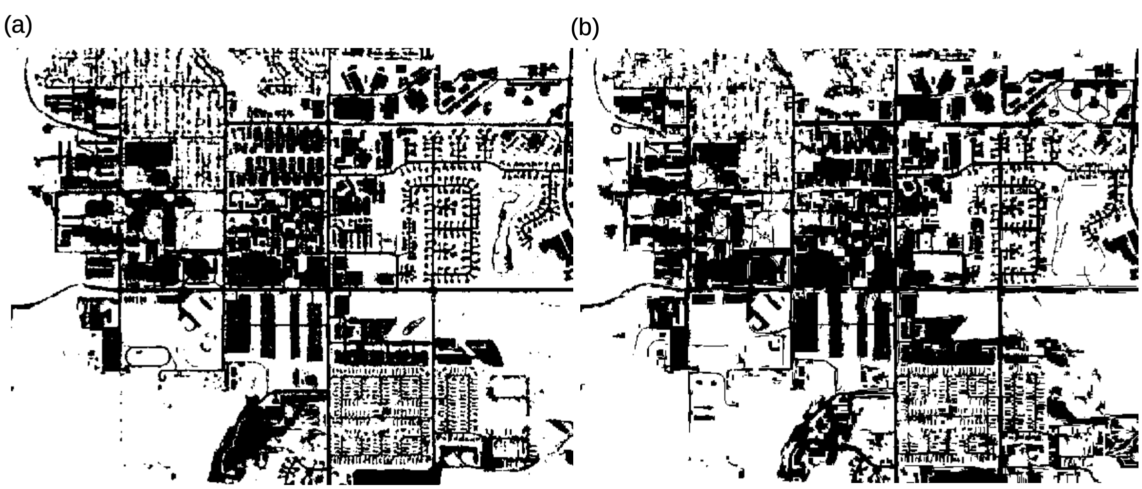

Figure 3. Final impervious surfaces derived from (a) maximum likelihood classification and (b) object-oriented classification.

CONCLUSIONS

The Quickbird imagery enabled mapping a complex urban area with high spatial variation. Comparing the per-pixel maximum likelihood classification to the object oriented approach, we found the object-based classification produces more homogeneous land cover classes with higher overall accuracy. This is an expected result since in high resolution imagery, each pixel is not related to the character of the object or area as a whole, but to the components within the object. Simple pixel-based classification may therefore be invalid. In addition, the object-oriented classification differentiates land cover classes based on not only the spectral information, but also spatial information of the image data. And, since it is based on fuzzy theory its classification result is more reasonable when dealing with mixed pixels that include more than one class (Baatz et al., 2004). Additionally, it is very convenient to refine the object-oriented classification result in eCognition given that the classification process is an iterative process. Nevertheless, for impervious surface mapping, the maximum likelihood classification performance seems better for delineating small impervious patterns such as the single-family residential buildings while object-based method tend to amalgamate impervious buildings and some surrounding lawn areas to the same object.

In object-oriented image analysis, multi-resolution segmentation separates adjacent regions in an image as long as they have significant contrast. Successful segmentation should create image objects that have optimal information for further extraction of land cover information. Our study confirms the outcome of image segmentation is directly related to the user defined parameters of scale and shape. Moreover, we found different land cover classes demonstrate different characteristics in relation to the modifications of scale parameter and shape factor, which makes quantitatively defining the optimal scale and shape factor an intricate task. Further studies are still needed in this regards.

While the high-resolution Quickbird imagery may provide the capability for mapping complex urban features in detail, there are still problems that make automatically extracting information from high-resolution data complicated. As pointed out by Niemeyer and Canty (2001), shadows and images with oblique or off-nadir view angles can cause false signals and unclear results. This study indicates shadow problem can be addressed partly by neighborhood analysis of per-pixel classification and with class-related features in object-based classification. However, it is almost unattainable to differentiate different types of shadows automatically because of the complicated fact that shadows include not only tree shadows, mostly occurring in pervious areas, but also building shadows that may occur in both pervious and impervious areas.

REFERENCES

Adams, J.B., D.E. Sabol, V. Kapos, R.A. Filho, D.A. Roberts, M.O. Smith, and A.R. Gillespie (1995). Classification of multispectral images based on fractions of endmembers: Application to land cover change in the Brazilian Amazon. *Remote Sensing of Environment*, 52:137-154.

Asner, G.P. and A.S. Warner (2003). Canopy shadow in IKONOS satellite observations of tropical forests and savannas. *Remote Sensing of Environment*, 87: 521–533.

Baatz, M., U. Benz, S. Dehghani, M. Heynen, A. Höltje, P. Hofmann, I. Lingenfelder, M. Mimler, M. Sohlbach, M. Weber, and G Willhauck (2004). *eCognition User Guide 4.* Definiens Imaging.

Bauer, M., N. Heinert, J. Doyle, and F. Yuan (2004). Impervious surface mapping and change monitoring using satellite remote sensing. In: *Proceedings, American Society of Photogrammetry and Remote Sensing Annual Conference*. May 24-28, 2004. unpaginated CD ROM, 10 pp.

Benz, U.C., P. Hofmann, G. Willhauck, I. Lingenfelder, and M. Heynen (2004). Multi-resolution object-oriented fuzzy analysis of remote sensing data for GIS-ready information. *ISPRS J. Photogrammetry and Remote Sensing*, 58:239-258.

Chan, J. C., K. Chan, and A.G. Yeh (2001). Detecting the nature of change in an urban environment: A comparison of machine learning algorithms. *Photogrammetric Engineering and Remote Sensing*, 67(2):213-225

Civco, D.L., J.D. Hurd, E.H. Wilson, C.L. Arnold, and M.P. Prisloe (2002). Quantifying and describing urbanizing landscapes in the Northeast United States. *Photogrammetric Engineering and Remote Sensing*, 68(10):1083- 1090.

Dougherty, M., R.L. Dymond, S.J. Goetz, C.A.Jantz, and N. Goulet (2004). Evaluation of impervious surface estimates in a rapidly urbanizing watershed. *Photogrammetric Engineering and Remote Sensing*, 70(11):1275-1284

Ji, M. and J.R. Jensen (1999). Effectiveness of subpixel analysis in detecting and quantifying urban imperviousness from Landsat Thematic Mapper imagery. *Geocarto International*, 14(4):33-41.

Lu, D. and Q. Weng (2004). Spectral mixture analysis of the urban landscape in Indianapolis city with Landsat ETM+ imagery, *Photogrammetric Engineering and Remote Sensing*. 70(9):1053-1062.

Niemeyer, I. and M.J. Canty (2001). Knowledge-based interpretation of satellite data for safeguards purposes by object-based and multi-scale image analysis. In: *Proceedings, 23rd Symposium on Safeguards and Nuclear Material Management, ESARDA 2001*, Bruges, Belgium, 8-10 May 2001.

Sawaya, K., L. Olmanson, N. Heinert, P. Brezonik. and M.Bauer (2003). Extending satellite remote sensing to local scales: Land and water resource monitoring using high-resolution imagery. *Remote Sensing of Environment*, 88:144-156.

Schueler, T.R. (1994). The importance of imperviousness. *Watershed Protection Techniques*, 1(3):100-110.

Schwarz M, Ch. Steinmeier and L. Waser (2000). Detection of storm losses in alpine forest areas by different methodic approaches using high-resolution satellite data. DEFINIENS eCognition website, http://www.definiens-imaging.com.

Small, C. (2003). High spatial resolution spectral mixture analysis of urban reflectance. *Remote Sensing of Environment*, 88:170–186.

Sun X. (2003). Comparison of pixel-based and object-oriented approaches to land cover classification using high-resolution IKONOS satellite data. Master's Thesis, University of Minnesota.

Wang, L., W. Sousa, and P. Gong (2004). Integration of object-based and pixel-based classification for mangrove mapping with IKONOS imagery. *International J. of Remote Sensing*, 25(24):5655-5668.

Willhauck G. (2000). Comparison of object-oriented classification techniques and standard image analysis for the use of change detection between SPOT multispectral satellite images and aerial photos. In: *Proceedings, ISPRS, Vol. XXXIII*.

Wu, C. (2004). Normalized spectral mixture analysis for monitoring urban composition using ETM+ imagery. *Remote Sensing of Environment*, 93:480-492.

Wu, C. and A. Murray (2003). Estimating impervious surface distribution by spectral mixture analysis, *Remote Sensing of Environment*, 84:493-505.

Yang, L., C.Huang, C.G. Homer, B.K. Wylie, and M.J. Coan (2003). An approach for mapping large-area impervious surfaces: synergistic use of Landsat-7 ETM+ and high spatial resolution imagery. *Canadian J. of Remote Sensing*, 29(2): 230- 240.

Yuan, F., M.E. Bauer, N.J. Heinert, and G. Holden. (2005). Multi-level land cover mapping of the Twin Cities (Minnesota) metropolitan area with multi-seasonal Landsat TM/ETM+ data. *Geocarto International*, 20(2):5-14.